

Modeling and System Identification of Autorotation Transitory of Rotorkite Experimental Setup

Future Scope of the Project:

This project is part of a bigger scope project called **Airborn Wind Energy Systems (AWE Systems)**. Its aim is to replace wind turbines by an innovative way to generate electricity and promises to be cheaper, more efficient and to occupy less space in the environment. The idea is to send drones flying in the air and tie them to a ground generator using a tether. The movement of the drones provides the rotational motion needed to generate electricity. The drones can reach much higher altitudes than wind turbines where the wind is stronger and more stable thus reaching higher efficiencies.

The project presented here however, is merely an experimental setup which does not fly nor generate electricity. It is a ground-fixed rotorkite setup whose blades rotate by the effect of wind blowing from a nearby electric fan. The setup is shown in **Figure 1** below.



Figure1: Rotorkite Experimental Setup

Section1: Introduction

(a) Explaining the Setup:

Three rotor blades are attached to the system using a swashplate. The swashplate is a device that is used in helicopters to convert translational motion to rotational motion by transmitting the pilot commands from the non-rotating part to the rotating rotor hub.

Figure 2 shows the swashplate assembly. Three servo motors control the movement of the blades. The swashplate allows two kinds of motion control (collective and cyclic). In this report, we define the controls of the system as:

$$u = [\delta_{col} \delta_{lat} \delta_{lon}] u = [\delta_{col} \delta_{lat} \delta_{lon}]$$

δ_{col} : collective pitch control -> controls the magnitude of the thrust vector

δ_{lat} : lateral pitch control -> controls the lateral orientation of the thrust vector

δ_{col} : cyclic pitch control -> controls the longitudinal orientation of the thrust vector

(b) Velocity Analysis:

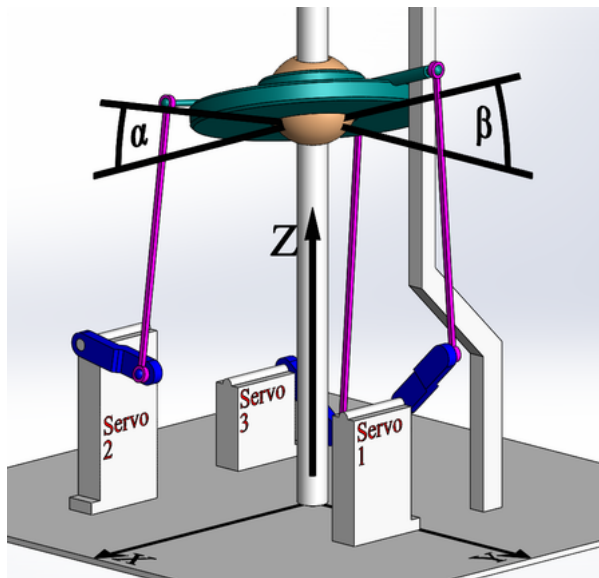


Figure2: Swashplate Assembly

Collective pitch control is when the swashplate is only allowed to move along the z-axis. Under collective pitch control, the position of the swashplate along the z-axis controls the magnitude of the pitch angle. This happens in such a way that the pitch angle is independent of angular position of the plates. This means that wherever the plate is during the revolution, it maintains a constant pitch angle. The collective pitch control is what determines the magnitude of the resulting thrust vector.

$$\theta = \delta_{col} + \delta_{lat} \cos(\psi) + \delta_{lon} \sin(\psi)$$

$$\delta_{lat} = 0$$

$$\delta_{lon} = 0$$

$$\theta = \delta_{col}$$

Cyclic Pitch Control allows the swash plate to tilt at an oblique angle. This affects the motion of the rotor blades by making the pitch angle dependent on the azimuthal position according to this equation. The cyclic pitch controls determine the orientation of the resulting thrust vector.

$$\theta = \delta_{col} + \delta_{lat} \cos(\psi) + \delta_{lon} \sin(\psi)$$

Section 2: Rotorkite Aerodynamics

This section provides a simplified analysis of the system's aerodynamics. Blade element analysis is used to analyze the velocity components of the blades which are used to determine the aerodynamic forces acting on the system. The goal of this section is to reach an ordinary differential equation that describes the behaviour of the system over time.

(a) Blade Element Analysis: The equations in this section are obtained from the Dissertation "Linear and Non-linear Control of Unmanned Rotorcraft". We refer to Chapter 4 regarding rotor dynamics. However, the dissertation is based on a helicopter. For our ground based rotorkite setup, we make two further simplifications.

1. That the wind blows in a direction perpendicular to the blades, thus the angle between the blades and wind is 90°.
2. The blades are fixed in such a way that they don't flap, so the flapping angle is ignored.

With reference to the rotorkite experimental system, we refer to three velocity components. Two are in-plane components acting in the plane where the rotors are rotating and one out-of-plane component acting in the direction of the wind blowing from the fan. Here, velocity refers to the relative velocity between the blades and the wind. In the horizontal direction for example, the free-stream wind velocity defines the out-of plane relative velocity component between the blades and the wind.

As defined in [1] these are velocity components and are shown in Figure 3 and Figure 4

U_P : out of plane velocity component that acts in the direction of the wind

U_T : tangential velocity component which causes the rotational motion of the blades. Since we refer to relative velocity, this component opposes the blade motion.

U_R : radial velocity component refers to how the freestream velocity acts on the radial axis of the blades. Since we assume the angle between the blades and wind direction is 90°, this component is assumed to be zero.

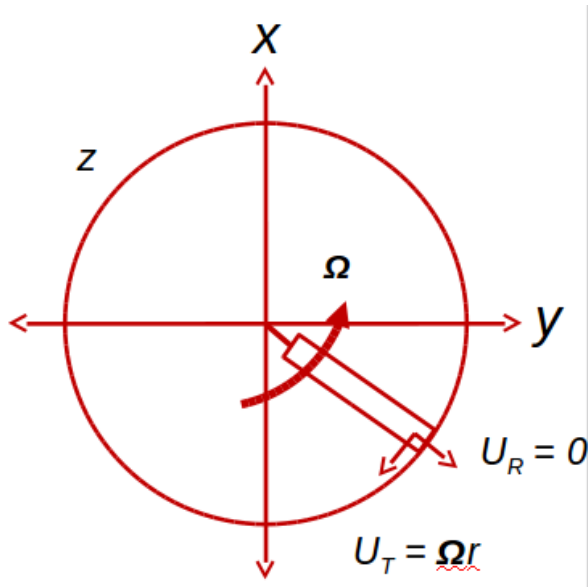


Figure3: Velocity Analysis in xy plane</h3

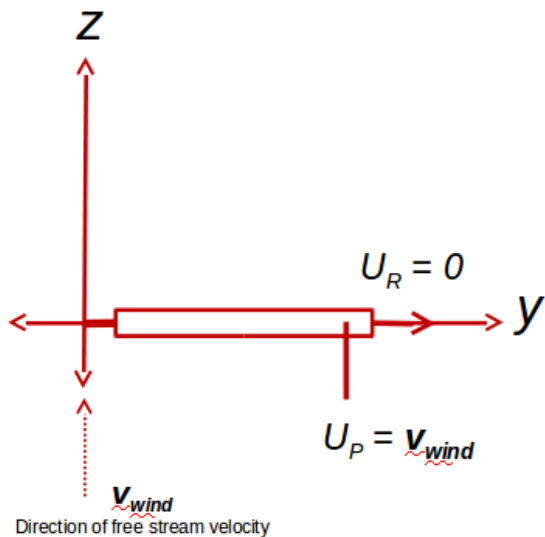


Figure4: Velocity Analysis in zy plane</h3

Blade element analysis is used to show how the velocity components act on the cross-section of the blades. The cross section is a 2D airfoil and the aerodynamic forces are calculated for each blade, then integration is done over the whole blade to obtain the total force acting on the system. The figures below shows the three velocity components are acting in the system.

$$U_R = 0$$

$$U_T = \Omega r$$

$$U_P = V_{WIND} + U_i$$

The resultant velocity is defined by:

$$U_{TOT} = \sqrt{U_T^2 + U_P^2}$$

Blade element analysis is done by studying how the The angle between U_{TOT} and the plane where the blades are located (x-y plane) is defined as: $\phi = \arctan \frac{U_P}{U_T}$ and is called the induced angle of attack

The angle of attack is defined as the angle between the line of chord of the airfoil and the relative velocity U_{TOT}

$$\alpha = \theta - \phi$$

The angles resulting from the above calculations are shown in **Figure6**.

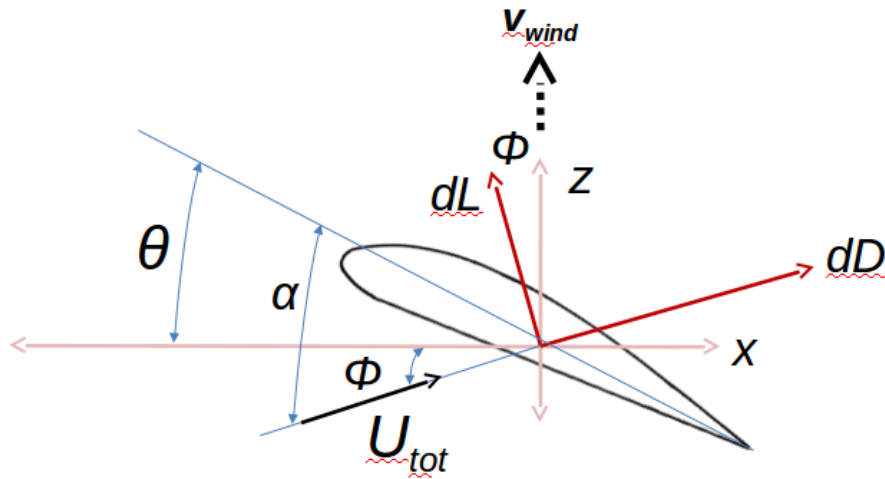


Figure5: Resulting angles

(b) Calculating Aerodynamic Forces:

After obtaining all the required velocity components and calculating the total relative velocity seen by the blade element, the aerodynamic forces are calculated. Lift force is the component of the force that is perpendicular to the flow direction. It is caused by the difference in pressure between the opposite sides of the blade. We use the following equation to define the incremental lift of one blade element.

$$dL = \frac{1}{2} \rho_a U^2 c_l \alpha dr$$

Drag force is the component of the force that acts parallel to the flow direction. It represents the the resistance to the relative movement between the blade and the air. Incremental drag is defined as following:

$$dD = \frac{1}{2} \rho_a U^2 c_d \alpha dr$$

The resultant of the incremental lift and drag forces that acts in the same plane of the blades is then calculated as

$$dF_x = dL \sin \phi + dD \cos \phi$$

By integrating this incremental force over the whole blade length, we obtain the total force

$$F_{TOT} = \int dF_x dr$$

The torque is then calculated as the total force multiplied by the blade radius

$$\tau = F_{TOT} R$$

The final step is then to obtain the ordinary differential equation.

$$\dot{\Omega} = I^{-1} \tau \text{ where } I \text{ is the moment of inertia}$$

Assuming the blade is long thin rod, its moment of inertia is define as:

$$I = \frac{1}{3} m L^2$$

Since the systems has 3 blades, final ode is given by:

$$\dot{\Omega} = (mL^2)^{-1} \tau$$

Which can be written in the standard form of

$$\dot{x} = h(x, u)$$

Where the state is $x = [\Omega]$ and the controls are $u = [\delta_{col} \delta_{lat} \delta_{lon}]$

Now this ode can be solved as an initial value problem.

Section 3: Using the Model to Analyze the Behaviour of the System:

This section presents the obtained plots showing how the system behaves over time. In the first part, we model using only collective pitch control. Assuming a certain swashplate position, we get a fixed pitch angle for each experiment run. The plot below shows how the rotational velocity varies over time. We observe how the system reaches the transitory state where Ω remains constant. Furthermore, at each pitch angle, a different steady state Ω is reached. We realize that the higher the pitch angle is, the lower is the steady state Ω . **Figure 6** shows the results of how Ω changes over time for 4 different pitch angles.

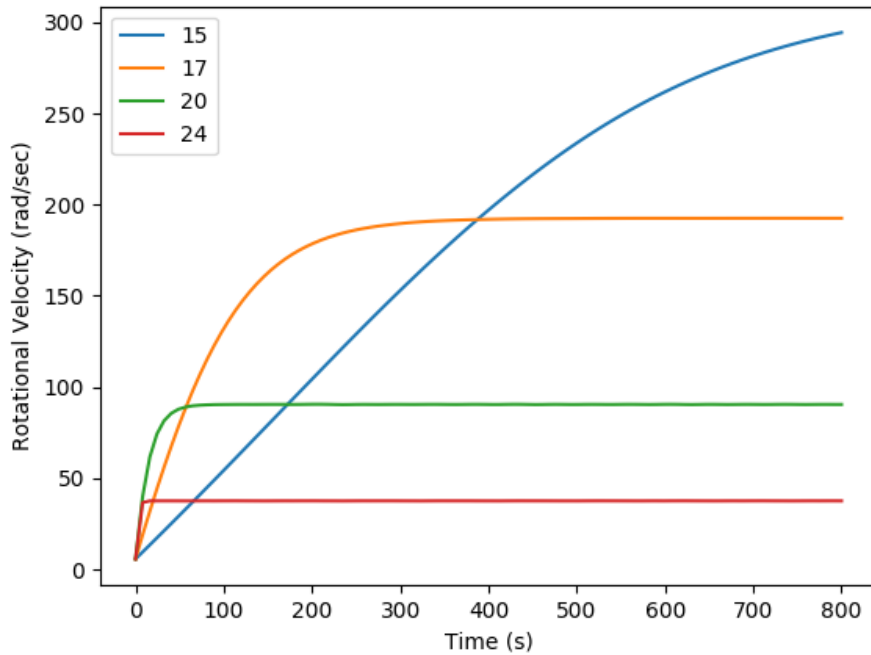


Figure6: How the rotational velocity varies over time

In the second run, we repeat the same setting, except that we larger blades. Here we also observe the trend of having a lower steady state at higher pitch angles, but overall we obtain lower rotational velocity values when using these larger blades.

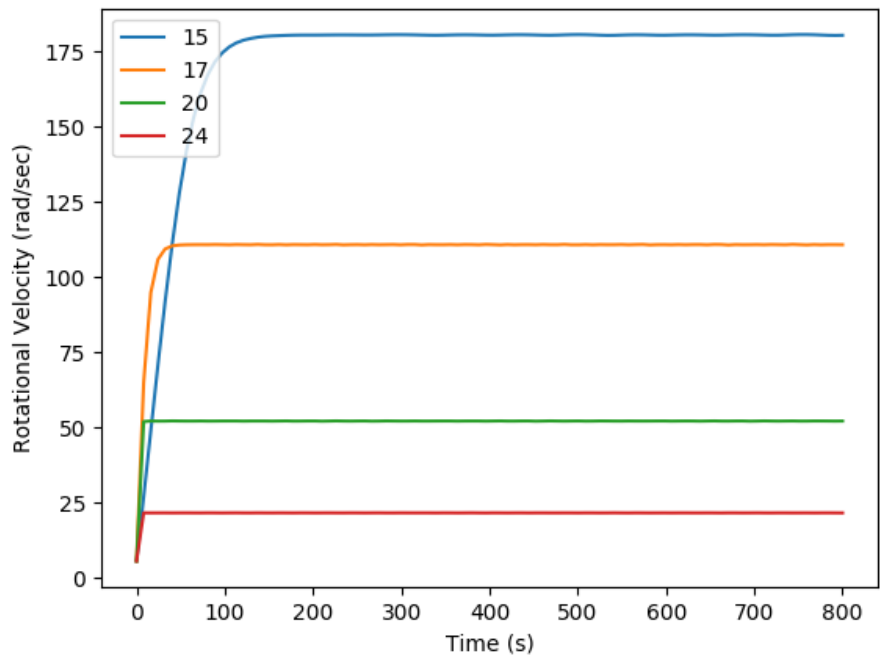


Figure7: Same Experiment repeated with larger Blades</h3

In the third run, we model both collective and cyclic pitch control. Now the pitch angle depends on the azimuthal position of the blade. We re-define the ode such that the states are now both the angular velocity and the azimuthal position.

$$x = [\Omega, \psi]$$

The relationship between the angular velocity and the azimuthal position is defined by:

$$\dot{\Omega} = \frac{d\psi}{dt}$$

And now the angle of attack calculation also differs because it depends on the pitch angle. The pitch angle, rather than being constant, is now defined by:

$$\theta = \delta_{col} + \delta_{lat} \cos(\psi) + \delta_{lon} \sin(\psi)$$

The obtained plots show that the angular velocity tends to approach a certain value, but is never constant and keeps fluctuating due to the cyclic pitch control.

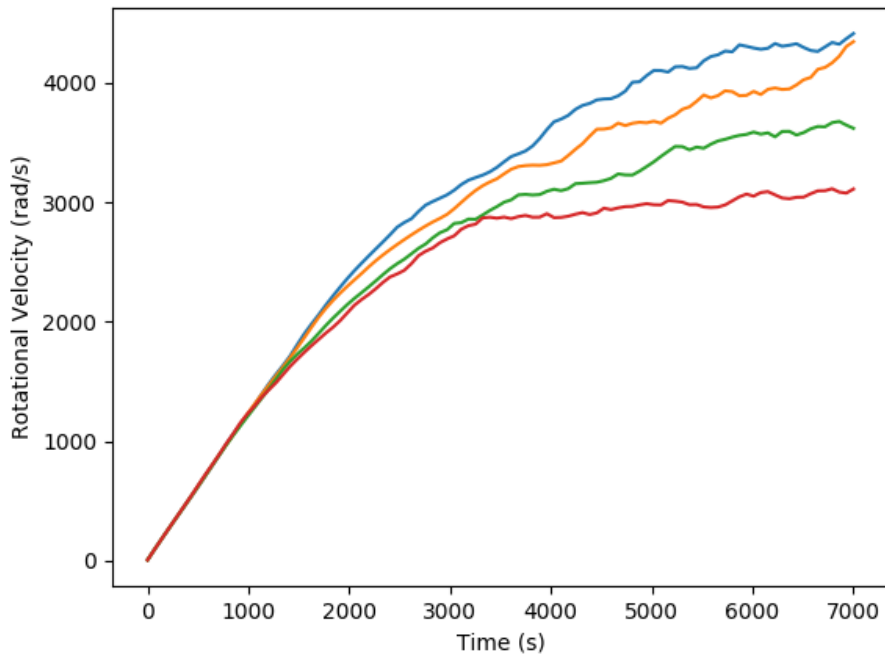


Figure8: Using cyclic and collective pitch control

Section 4: Running Tests on the Real Rotorkite Experimental Setup

Now the tests are performed on the real system. The electric fan is turned on to observe and collect data about how the wind blowing causes the blades to rotate. The initial angular velocity of the blades is always set to zero. The tests are done assuming only collective pitch controls and are repeated for both short and long blades. The following plots are obtained

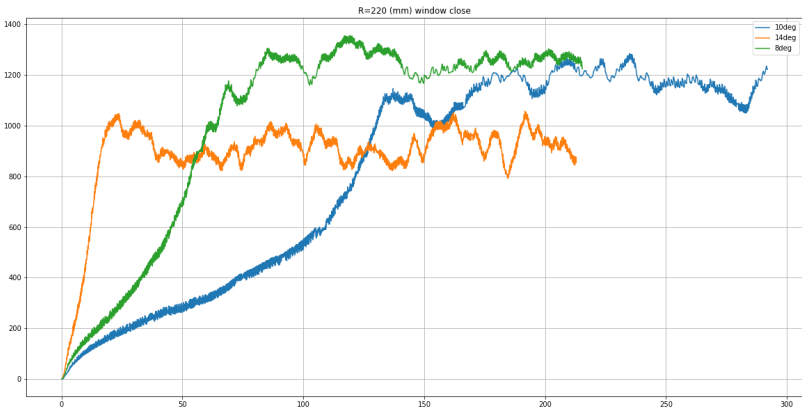


Figure9: Experiment on the real setup</h3

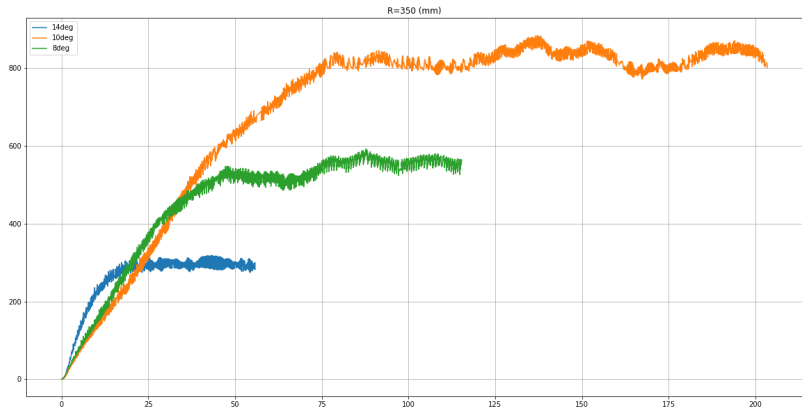


Figure10: Same as Figure 5 but using larger blades</h3

Section 5: Final Discussion and Results

By comparing the results from the model and the real setup which were presented in sections 2 and 3 respectively, we observe that the real data resembles the model more closely when the model included both cyclic and collective pitch control. Although in the real experiment we assumed only collective pitch control where the swashplate was kept vertical with no tilting, the results suggest that this constraint was not satisfied in the real experiment. Maybe the swashplate was tilting even though the cyclic pitch controls were set to zero. This also calls for the need of a more accurate measurement of the exact values of pitch angle and cyclic and collective pitch controls. Furthermore, the results from the model and real setup seem to match well in terms of having lower steady state Ω at higher pitch angle values and when smaller blades are used.

Section 6: Current Limitations and Future Work:

-In finding a preliminary model of the system, we ignored the inflow velocity which should have appeared in the equations of U_P in section 2. A more accurate model is required to obtain better results.

-The lift and drag coefficients used in the system are only accurate for small angles of attack. Therefore, we should limit the system to only a small range of angle of attack values

Section 7: Further Extensions on the Project

(a) Observing how the angle of attack values vary during the experiment The jupyter-notebook `aoa.ipynb` shows how the angle of attack varies during the experiment. The first graph shows how it varies between origin (rotor-hub), blade middle point and blade tip. The second graph shows how it varies for different pitch angles.

(b) Modeling how the blades disturb the flow of the wind coming from the fan

In the previous experiments, we ignored the effects of the inflow velocity. In reality the flow of the wind is disrupted by the rotating blades. When taking this effect into account. There exists several methods to calculate the inflow velocity. These methods include vortex theory and momentum theory. The calculations presented below aim to include this disruption of the below in the system analysis.

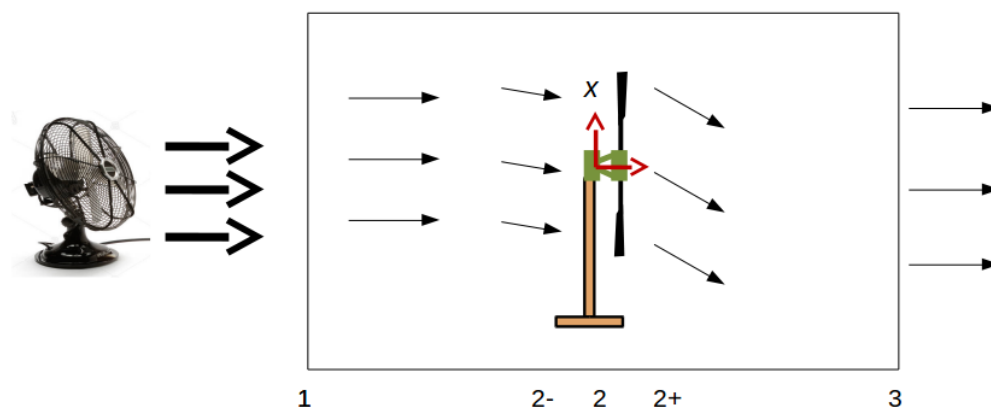


Figure11: Schematic diagram showing effect of inflow velocity

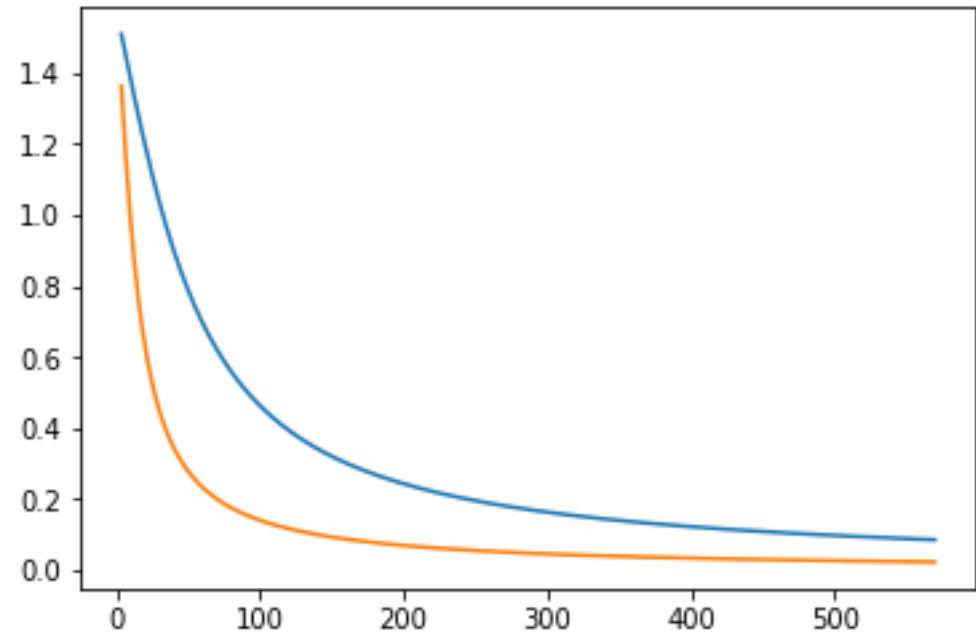


Figure12: Angles of attack along the blade

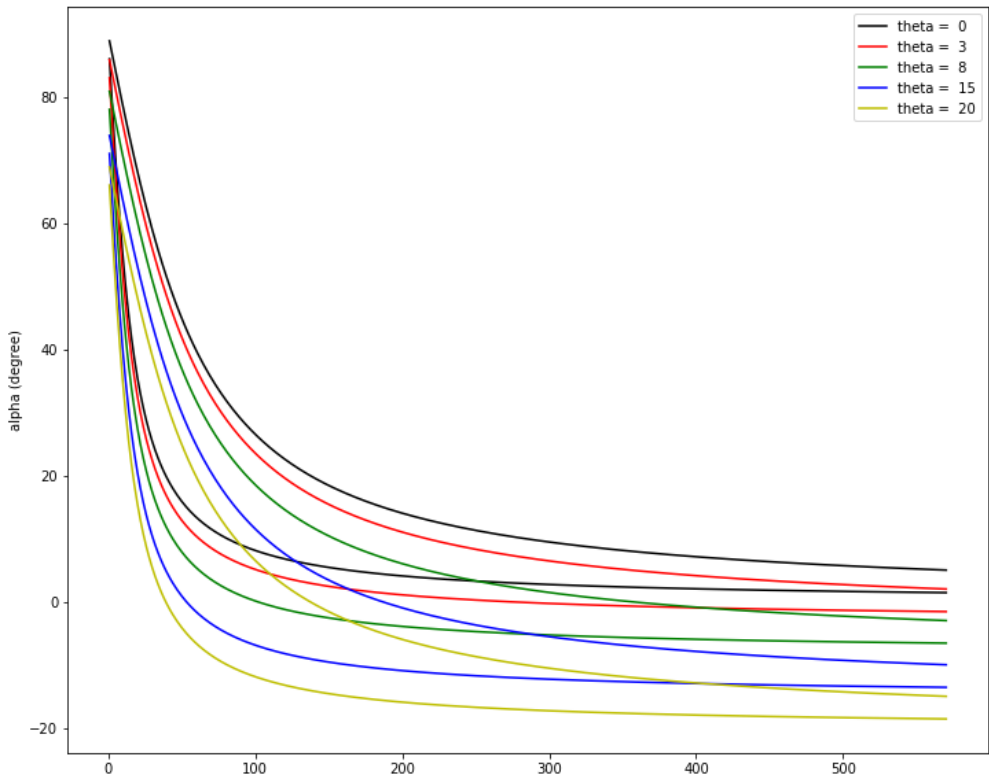


Figure13: Angles of attack along the blade at differnt pitch angles

Assumptions:

$$\hat{n} \times u_{\infty} = 0$$

$$P_1 = P_3$$

$$u_2^+ = u_2^-$$

Conservation of Mass:

$$\dot{m}_1 = \dot{m}_2 = \dot{m}_3$$

$$\rho u_1 A_1 = \rho u_2 A_2 = \rho u_3 A_3$$

Bernoulli:

$$P_1 + \frac{1}{2}\rho(u_1)^2 = P_2 + \frac{1}{2}\rho(u_2^+)^2$$

$$P_2 + \frac{1}{2}\rho(u_2^-)^2 = P_3 + \frac{1}{2}\rho(u_3)^2$$

Newtons Second Law: force = change in momentum

$$F = \Delta M$$

$$F + u_3 \dot{m} = u_1 \dot{m}$$

$$Pressure = \frac{Force}{Area}$$

$$F = (P_2^+ - P_2^-)A$$

$$F = u_1 \dot{m} - u_3 \dot{m} = (P_2^+ - P_2^-)A$$

$$F = A(P_1 + \frac{1}{2}\rho u_1^2 - \frac{1}{2}\rho u_{2^+} - P_3 - \frac{1}{2}\rho u_3^2 + \frac{1}{2}\rho u_{2^-})$$

$$F = A\frac{1}{2}\rho(u_1^2 - u_3^2)$$

Resulting Equation:

$$\frac{1}{2}(u_1^2 - u_3^2) = u_2(u_1 - u_3)$$

$$\frac{1}{2}(u_1 - u_3)(u_1 + u_3) = u_2(u_1 - u_3)$$

$$(u_1 + u_3) = 2u_2(u_1 - u_3)$$

$$u_3 = 2u_2 - u_1$$

Induction Factor a:

$$a = \frac{u_1 - u_2}{u_1}$$

$$u_2 = -u_1 a + u_1$$

$$u_2 = u_1(1 - a)$$

$$u_3 = 2u_1(1 - a) - u_1$$

$$u_3 = 2u_1 - 2u_1 a - u_1$$

$$u_3 = u_1(1 - 2a)$$

$$CT = \frac{F}{A(\frac{1}{2}\rho u_1^2)}(u_1 - u_3)$$

$$CT = \frac{2u_1(1-a)(u_1 - u_1(1-2a))}{u_1^2}$$

$$CT = 2(1 - a)(2a)$$

$$CT = 4a(1 - a)$$

$$4a^2 - 4a + CT = 0$$

$$a = \frac{1}{2} + / - \frac{1}{2}\sqrt{1 - CT}$$

Feasible Answer is given when the negative solution is chosen

$$a = \frac{1}{2}(1 - \sqrt{1 - CT})$$

$$\vec{u}_i = -a\vec{u}_\infty$$

$$\vec{u}_i = -\frac{1}{2}(1 - \sqrt{1 - CT})\vec{u}_\infty$$

References:

[1] Raptis, I., & Valavanis, K. (2011). Linear and nonlinear control of small-scale unmanned helicopters. Dordrecht: Springer.

Acknowledgement:

This project was done under the supervision of Tommaso Sartor. Sincere thanks are extended to him for his continuous guidance throughout the semester. Furthermore, we would like to thank Rachel Leuthold for her input regarding how to model the inflow velocity.